

## Crystal Field and Site Symmetry of Trivalent Cerium Ions in $\text{CaF}_2$ : The $C_{4v}$ and $C_{3v}$ Centers with Interstitial-Fluoride Charge Compensator\*

W. J. Manthey†

*Department of Physics, University of Chicago, Chicago, Illinois 60637*

(Received 15 March 1973; revised manuscript received 11 July 1973)

Optical spectra of two  $\text{Ce}^{3+}$  impurity centers in  $\text{CaF}_2$  are described. The centers are those with charge compensation by  $\text{F}^-$  ions at the two interstitial sites nearest to the  $\text{Ce}^{3+}$  ion, one site in the direction of a  $C_4$  axis of the lattice and the other site in the direction of a  $C_3$  axis. The ultraviolet absorption and fluorescence spectra of the first,  $C_{4v}$ , center are described and analyzed in terms of crystal-field theory. The four broad absorption bands from the  $4f \rightarrow 5d$  transitions are assigned to the  $e$  and  $t_2$  levels, and the splitting in the complete  $C_{4v}$  crystal field is used to determine the  $5d$  crystal-field parameters. From first-order  $4f$  and  $5d$  wave functions, the oscillator strength of the lowest-energy absorption band is predicted and is found to agree well with the measured value. The fluorescence spectrum of a low-concentration crystal of  $\text{CaF}_2:\text{Ce}^{3+}$  at liquid-helium temperature is described and found to arise mostly from transitions from the lowest  $5d$  level of the  $C_{4v}$  center to the  $4f$  levels as split by the  $C_{4v}$  crystal field. Vibrational sidebands of several of the zero-phonon lines in fluorescence are found to agree in detail with the vibrational sideband of the lowest-energy absorption line. Six of the seven  $4f$  levels of the  $C_{4v}$  center are assigned, and from them, in combination with  $g$  factors of the ground state, are determined the  $4f$  crystal-field parameters and the exact  $4f$  wave functions. Transition probabilities predicted from these quantities agree with the observed line strengths in fluorescence. A very closely spaced pair of lines near  $3118.5 \text{ \AA}$  is observed in some  $\text{CaF}_2:\text{Ce}^{3+}$  samples and is attributed to the second,  $C_{3v}$ , center. Support for this comes from the comparison of these lines and their hot band with the corresponding absorption in the oxide-compensated  $C_{3v}$  center of  $\text{CaF}_2:\text{Ce}^{3+}$  and from their behavior under uniaxial stress.

### I. INTRODUCTION

Many investigators have published observations of the behavior of the trivalent cerium ion as an impurity ion in the  $\text{CaF}_2$  lattice. This system is an attractive one for study because  $\text{Ce}^{3+}$  possesses a single optically active electron, whose  $4f$  orbital, like those of the other rare-earth ions, is acted on only weakly by external fields. The rare-earth ion readily substitutes for a  $\text{Ca}^{++}$  ion of the lattice, leaving it in a crystalline environment easy to visualize, with the greatest crystal field contribution of the lattice coming from the eight nearest-neighbor fluoride ions.

In contrast to the expected simplicity of the optical properties of the  $\text{CaF}_2:\text{Ce}^{3+}$  system, close investigation, in particular of the ultraviolet absorption at liquid-helium temperatures and high resolution, presents difficulties in interpretation. The multitude of absorption lines in regions where only one or two are expected indicates that the system is not as simple as anticipated. These difficulties have been correctly attributed<sup>1</sup> to the simultaneous presence of a plurality of cerium centers of different site symmetry.

In the cerium centers treated here, charge compensation of the  $\text{Ce}^{3+}$  substitutional ion is by a close-lying interstitial  $\text{F}^-$  ion. Figure 1 shows part of the pure  $\text{CaF}_2$  lattice, with a  $\text{Ca}^{++}$  ion at the origin, surrounded by eight  $\text{F}^-$  ions and twelve other  $\text{Ca}^{++}$  ions. The lattice constant  $a$  is  $5.447 \text{ \AA}$  at  $77 \text{ K}$ .<sup>2</sup>

When a  $\text{Ce}^{3+}$  ion substitutes for the central  $\text{Ca}^{++}$  ion, a charge-compensating interstitial  $\text{F}^-$  ion can be inserted, without grossly distorting the lattice, at  $(\frac{1}{2}a, 0, 0)$ , at  $(\frac{1}{2}a, \frac{1}{2}a, \frac{1}{2}a)$ , or at any one of an infinity of similar, more distant sites. Figures 2 and 3 show the first two of these  $\text{Ce}^{3+}$  centers. The  $O_h$  (cubic) symmetry of the  $\text{Ca}^{++}$  site has been changed to the lower symmetries,  $C_{4v}$  (tetragonal) and  $C_{3v}$  (trigonal), respectively, of the  $\text{Ce}^{3+}$  sites.

The ultraviolet absorption spectrum of a  $\text{CaF}_2$  crystal which contains a low concentration of  $\text{Ce}^{3+}$  ions as an impurity consists of six or seven broadbands between  $3390$  and  $1850 \text{ \AA}$  attributable<sup>3</sup> to  $4f \rightarrow 5d$  transitions in the  $\text{Ce}^{3+}$  ions. Likewise in fluorescence, the bands observed between  $3130$  and  $3540 \text{ \AA}$  can be attributed to  $5d \rightarrow 4f$  transitions in the  $\text{Ce}^{3+}$  ions. The cerium center responsible for most of these bands (see below) is the  $C_{4v}$  center of Fig. 2, or, more precisely, a  $C_{4v}$  center differing from that in Fig. 2 only by small displacements of some of the ions, which do not alter the symmetry.<sup>4</sup>

Interpretation of the absorption spectrum of the  $C_{4v}$  center in terms of its crystal-field splitting of the  $5d$  orbital has up until now not been entirely satisfactory, and therefore this paper will reexamine this problem. New observations will also be reported of the fluorescence of the  $C_{4v}$  center, and from them the crystal field acting on the  $4f$  orbital will be worked out.

Among the numerous sharp lines that occur in

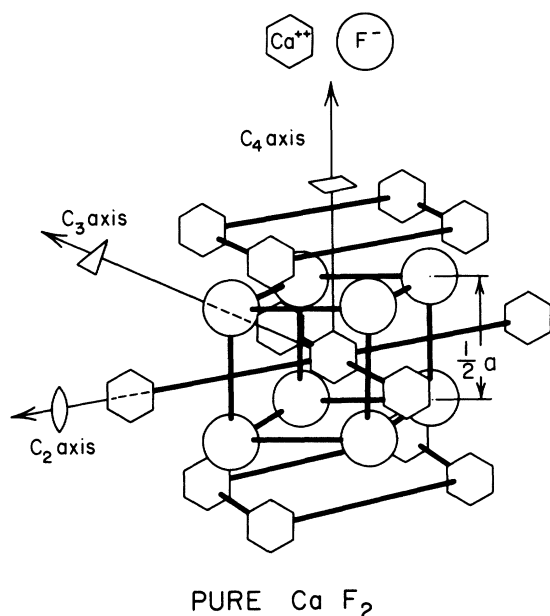


FIG. 1. Structure of the  $\text{CaF}_2$  lattice, showing that the  $\text{Ca}^{++}$  sites have  $O_h$  symmetry. The eight nearest-neighbor  $\text{F}^-$  sites and the 12 next-nearest-neighbor  $\text{Ca}^{++}$  sites are shown.

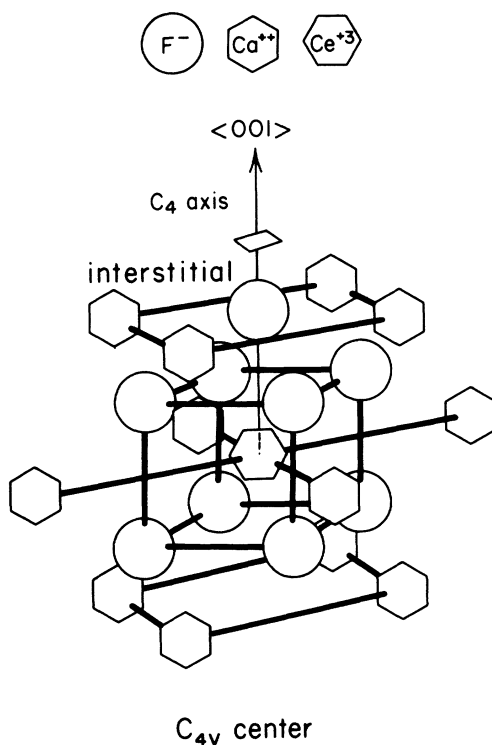


FIG. 2.  $C_{4v}$  center of  $\text{CaF}_2:\text{Ce}^{3+}$ . The  $\text{Ce}^{3+}$  ion substitutes for a  $\text{Ca}^{++}$  ion, while an interstitial  $\text{F}^-$  ion at (approximately) the center of one of the nearest empty cubes of lattice  $\text{F}^-$  ions reduces the point symmetry of the  $\text{Ce}^{3+}$  ion to  $C_{4v}$ .

the absorption spectrum of  $\text{CaF}_2:\text{Ce}^{3+}$  when the temperature approaches that of liquid helium, a pair of very close-lying lines has been observed in the region of the lowest-energy absorption lines of the  $C_{4v}$  center. Evidence will be presented here to support the assignment of these lines to the  $C_{3v}$  center with charge compensation by an interstitial  $\text{F}^-$  ion as shown in Fig. 3. Later papers in this series will describe observations and interpretations of the absorption spectra of other cerium centers in  $\text{CaF}_2$  with a variety of crystal fields and site symmetries, in particular those where charge compensation of the  $\text{Ce}^{3+}$  ion is by ions other than an interstitial  $\text{F}^-$  ion.

## II. EXPERIMENTAL METHODS

The samples used in this study were single crystals of  $\text{CaF}_2$  doped with  $\text{CeF}_3$ , grown by the gradient-freeze method under a flow of a mixture of 0.1-ft<sup>3</sup>/h helium and 0.01-ft<sup>3</sup>/h hydrogen fluoride. After crystallization was complete, the crystals were annealed in an atmosphere of hydrogen fluoride. The  $\text{CaF}_2$  was acquired in the form of high-purity "chips" from the Harshaw Co.

Absorption spectra at liquid-nitrogen temperature were observed on a Cary 14 spectrophotometer, using a cryostat with fused-quartz windows. Absorption and fluorescence spectra at liquid-helium temperatures were observed on a Jarrell-Ash 3.4-m spectrograph, using the first-order

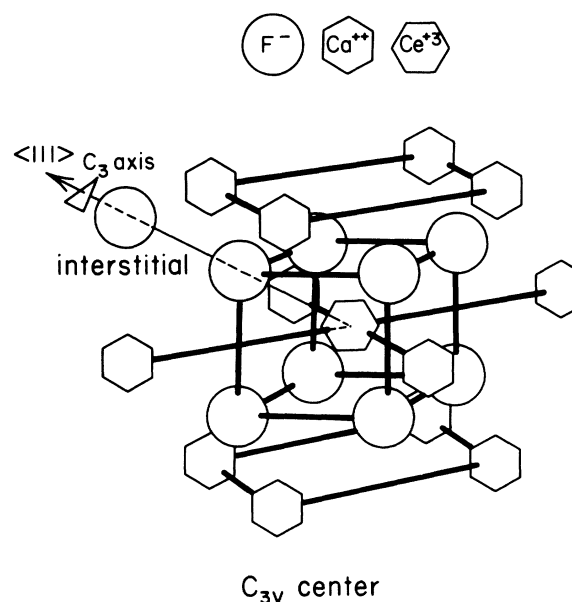


FIG. 3. The  $C_{3v}(F_i^-)$  center of  $\text{CaF}_2:\text{Ce}^{3+}$ . Here the interstitial  $\text{F}^-$  ion is at (approximately) the center of one of the next-nearest empty cubes of lattice  $\text{F}^-$  ions, and reduces the point symmetry of the  $\text{Ce}^{3+}$  ion to  $C_{3v}$ .

diffraction from an Ebert-mounted 30 000-line/in. grating.

The exciting light for fluorescence came from a high-power xenon arc, and then passed through either a quarter-meter Bausch and Lomb monochromator or a series of filters. Since the emitted light had to pass through the crystal to reach the spectrometer, the resonance line at 3131.7 Å was reabsorbed and so does not appear. The emission was readily detected both photoelectrically and photographically, but the weakest lines showed up only on the photographic plates.

For observing splitting produced by uniaxial strain, a rectangular parallelepiped with top and bottom (001) faces each about 0.267 cm<sup>2</sup> in area was cut from a crystal of CaF<sub>2</sub>:Ce<sup>3+</sup> (0.003 mole %). The strain apparatus was essentially the same as that described by Meltzer<sup>5</sup> except for being slightly larger.

### III. ABSORPTION OF THE C<sub>4v</sub> CENTER

Figure 4 shows the absorption spectrum between 3320 and 1850 Å of a typical oxygen-free crystal of low-concentration CaF<sub>2</sub>:Ce<sup>3+</sup> at liquid-nitrogen temperature. The six broad absorption bands are lettered B–G. Crystals contaminated with oxygen also show a band A, arising from trigonal oxide-compensated centers, described briefly in Sec. V.

The absorption of CaF<sub>2</sub>:Ce<sup>3+</sup> has been studied by Loh,<sup>7</sup> using a vacuum spectrometer to attain wavelengths as low as 1240 Å. He used a series of crystals with cerium doping varying from 0.005 to 5 mole% and found that the absorbance of bands B, E, F, and G increased considerably more slowly with cerium concentration than did that of bands C and D. From this fact he correctly concluded that bands B, E, F, and G arose from a different center than did bands C and D. These last two bands are usually called cluster bands on the assumption that they arise from clusters of two or more Ce<sup>3+</sup> ions.

This leaves bands B, E, F, and G as the absorption bands of the predominating single-ion Ce<sup>3+</sup> center, namely (see below), the C<sub>4v</sub> center. Their spacing should be that of the 5*d* energy levels. Theory predicts that there are five of these levels, split by the C<sub>4v</sub> crystal field and by the spin-orbit interaction, so that the only remaining degeneracy is Kramer's degeneracy. Figure 5 shows the expected energy-level diagram. Setting aside the possibility that one of the bands B, C, D, E, F, or G arises from two overlapping levels, it seems, therefore, that one level is missing.

The interpretation offered here is that this missing level is the second-lowest, *deGE*<sub>1/2</sub> in Fig. 5, and that it fails to appear because the correspond-

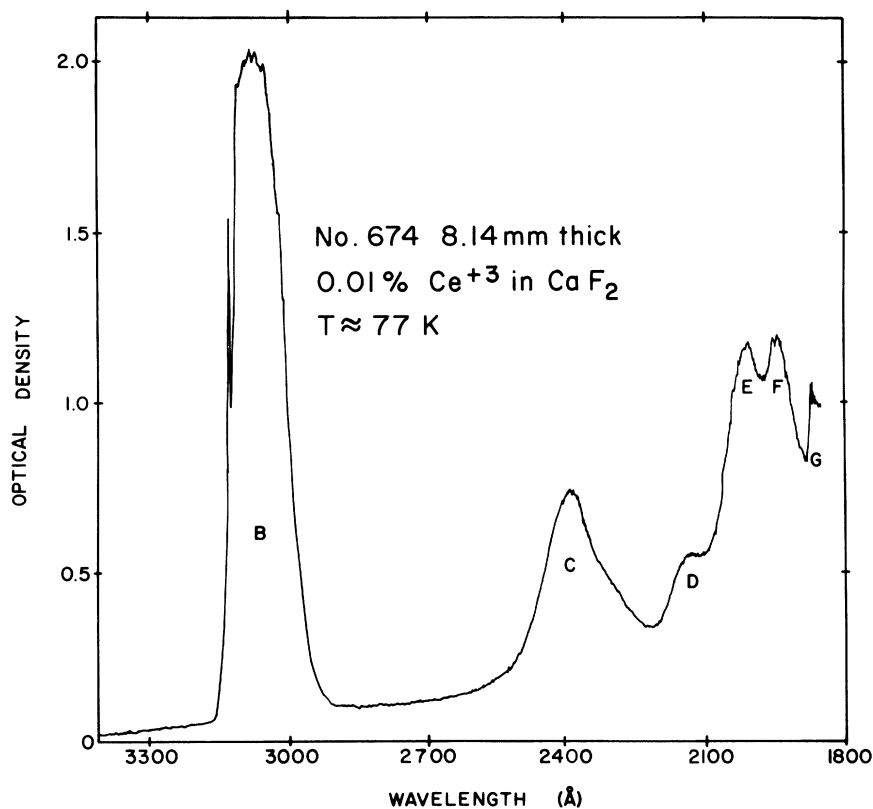


FIG. 4. Absorption spectrum at liquid-nitrogen temperature of CaF<sub>2</sub>:Ce<sup>3+</sup> (0.01 mole%), recorded on a Cary 14, and showing bands B–G.

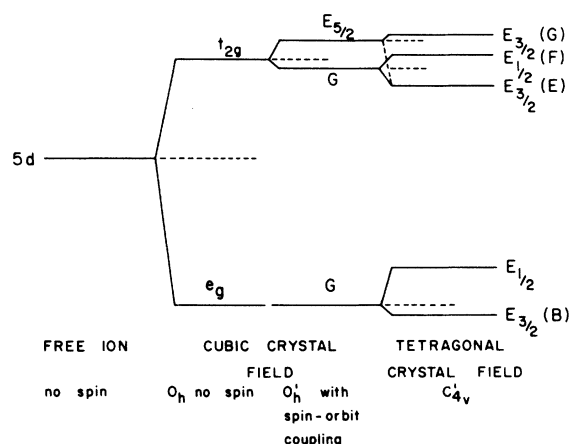


FIG. 5. Energy levels of the  $5d$  orbital of  $Ce^{3+}$  as split by the crystal field of the  $C_{4v}$  center plus spin-orbit coupling.

ing transition probability is too small. A first-order calculation, using the wave functions of the lowest  $4f$  and the two lowest  $5d$  states, gives the result that this transition has a strength 0.04 times that to the lowest energy level,  $deGE_{3/2}$ , corresponding to band B. Attempts were made during the course of the present experiments to find this weak band, but they were unsuccessful.<sup>6</sup>

Loh's<sup>7</sup> assignment of bands B, E, F, and G to the  $5d$  energy levels of the  $C_{4v}$  center was in error. First he assumed that spin-orbit splitting of the  $t_2$  energy levels was negligible, with the result that levels  $dt_2GE_{1/2}$  and  $dt_2E_{5/2}E_{3/2}$  (see Fig. 5) were predicted to be degenerate. In fact, however, the spin-orbit splitting is small only with respect to the *over-all* crystal-field splitting, or with the cubic-field part of it—that is, the splitting of the  $e$  levels from the  $t_2$  levels. Instead of being negligible, one can expect the spin-orbit splitting of the  $t_2$  levels to amount to some  $\frac{3}{2}\zeta_{5d} \approx 1500 \text{ cm}^{-1}$ ; this splitting should be easy to detect.

Next, Loh identified bands B and E with the two  $e$  levels split by the low-symmetry part of the  $C_{4v}$  crystal field, leaving bands F and G to represent the  $t_2$  levels. In fact, however, splitting of the  $e$  levels upon reduction of symmetry  $O_h \rightarrow C_{4v}$  can confidently be predicted to be almost an order of magnitude smaller than the splitting, in a crystal field of  $O_h$  symmetry, of the  $e$  levels from the  $t_2$  levels. Even the simple point charge model, which is expected to give too high an estimate of the low-symmetry part of the  $C_{4v}$  crystal field, predicts only about  $6800 \text{ cm}^{-1}$  for the splitting between the  $deGE_{3/2}$  and  $deGE_{1/2}$  levels of Fig. 5. This puts them much closer together than the  $e$ - $t_2$  separation.

Accordingly, since bands B and E seem much

too far apart to correspond to the two  $e$  levels, it is more acceptable to assign bands E, F, and G to the three expected  $t_2$  levels, leaving only band B to represent one (or conceivably both) of the two expected  $e$  levels. Table I lists the observed positions of the absorption bands (band A is included for completeness) along with the assignments of bands B, E, F, and G to the expected levels shown in Fig. 5. Details of the analysis of the  $5d$  levels of the  $C_{4v}$  center are presented elsewhere.<sup>8</sup> This analysis results in values, also presented in Table I, for the crystal-field parameter  $B_0^4$  and a spin-orbit parameter  $\zeta_{5d}$ , different from the free-ion value<sup>9</sup> of  $995.6 \text{ cm}^{-1}$ . Notice that the value of  $B_0^4$  in Table I is equivalent to  $Dq = 1700 \text{ cm}^{-1}$ , considerably larger than the value found by Loh.<sup>7</sup>

Manual integration of band B gives an experimental value of the oscillator strength of  $f = 4.30 \times 10^{-3}$ . Using the Hartree-Fock radial wave functions for cerium,<sup>10</sup> the predicted value of this quantity is  $f = 5.86 \times 10^{-3}$ . The agreement is seen to be adequate, although the value obtained by Wagner and Mascarenhas by the method of ionic thermocurrents<sup>11</sup> is about three times as great, perhaps because of a different distribution of  $Ce^{3+}$  ions over centers of different symmetries. Unfortunately, agreement between predicted and observed values of  $f$  for absorption bands E, F, and G is considerably less satisfactory. This may result from the fact that the windows of the cryostat have a fairly high absorbance in this wavelength region.

At liquid-helium temperature, band B shows a great deal of fine structure—in particular, a number of sharp (zero-phonon) lines in addition to the most prominent one, on the low-energy side of band B, at  $3131.7 \text{ \AA}$ . The other lines may vary in number and strength from one sample to another. Accordingly, it has not been possible, except in the case of the very closely spaced doublet at  $3118.5 \text{ \AA}$  observed in some crystals and described in Sec.

TABLE I. Absorption bands of  $Ce^{3+}$  in  $CaF_2$  at liquid-nitrogen temperature and crystal-field parameters of the  $5d$  configuration of the  $C_{4v}$  center.

Band	$\lambda$ ( $\text{\AA}$ )	$\sigma$ ( $\text{cm}^{-1}$ )
A	3290	30 390
B	3190	31 340
C	2407	41 530
D	2135	46 820
E	2020	49 490
F	1954	51 160
G	1873	53 370
$\zeta_{5d} = 1305.5 \text{ cm}^{-1}$		
$B_0^4 = -36 600 \text{ cm}^{-1}$		

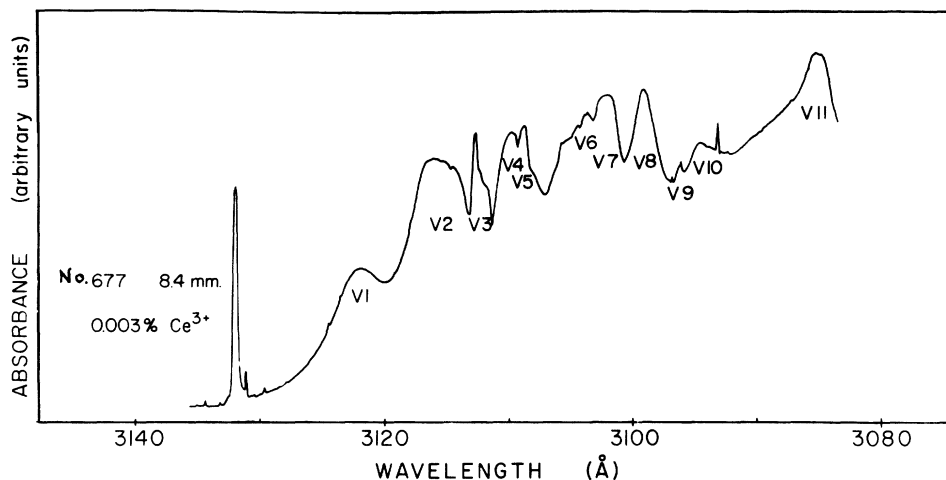


FIG. 6. Absorption spectrum at liquid-helium temperature of a  $\text{CaF}_2:\text{Ce}^{3+}$  crystal, showing line  $C_{4v}$ ,  $DeGe_{3/2}$ , its vibrational sideband, and other lines in this region. Thickness and nominal doping per mole with  $\text{CeF}_3$  as noted. Photoelectric recording from Jarrell-Ash 3, 4-m spectrometer. Arbitrary labels have been assigned to components of the vibrational sideband.

V and of a few other lines to be described in the later papers of this series, to determine how they depend on the conditions of preparation of the crystal. The absorption spectrum at liquid-helium temperature shown in Fig. 6 has about as few of these additional lines as are found in any of the samples studied, while it clearly shows the strong, sharp line at  $3131.7 \text{ \AA}$ , representing the zero-phonon line of band B.

In addition to their earlier work<sup>3</sup> on this line and related spectra, Kaplyanskii and his co-workers used the effects of applied electric fields<sup>12</sup> and uniaxial stress<sup>13</sup> to show that it arose from a center with tetragonal symmetry, and that the crystal quantum number of both the excited and the ground state was the same—namely,  $\mu = \pm \frac{3}{2}$  (equivalent to our assignment here of the states to irreducible representation  $E_{3/2}$  of group  $C_{4v}$ ). Observations of the Zeeman splitting of the line at  $3131.7 \text{ \AA}$  by Crozier<sup>14</sup> also showed tetragonal symmetry, although the crystal quantum number of the upper state was incorrectly assigned.

That the  $C_{4v}$  center is the predominating cerium center in oxygen-free  $\text{CaF}_2:\text{Ce}^{3+}$  has been unambiguously shown by electron-nuclear-double-resonance (ENDOR) measurements,<sup>4,15</sup> while several earlier investigations by EPR led to the same interpretation.<sup>16</sup> Theoretical considerations led Heist and Fong to predict<sup>17</sup> this predominance of the  $C_{4v}$  center at temperatures below 970 K. In connection with the  $C_{3v}$  center giving rise to the spectrum described in Sec. V, it may be pointed out that Heist and Fong's model predicted that the second most probable of the  $\text{Ce}^{3+}:\text{F}_i^-$  centers ( $\text{F}_i^-$  is the interstitial  $\text{F}^-$  ion) would be, at all temperatures, not the one with the second-smallest  $\text{Ce}^{3+}:\text{F}_i^-$  spacing, but rather that with the third-smallest  $\text{Ce}^{3+}:\text{F}_i^-$  spacing. The latter is a center of  $C_s$  symmetry with  $\text{F}_i^-$  at  $(a, \frac{1}{2}a, 0)$ , which, ac-

cording to this model, predominates over the  $C_{3v}$  center with  $\text{F}_i^-$  at  $(\frac{1}{2}a, \frac{1}{2}a, \frac{1}{2}a)$ .

An attempt was made to detect a hot band of the line at  $3131.7 \text{ \AA}$  by observing the absorption at greater wavelengths with the temperature slowly varying from 2.2 to 51.5 K, and at 77 K. That no such hot band appears suggests that the second-lowest  $4f$  level of the  $C_{4v}$  center lies higher than  $50 \text{ cm}^{-1}$ . Measurement of spin-lattice relaxation<sup>18</sup> indicates that this level ought to lie a few hundred  $\text{cm}^{-1}$  above the ground level. Fluorescence also fails to show directly the position of this level, but calculations from the positions of the other  $4f$  levels revealed by fluorescence suggest (see below) that it lies at about  $110 \text{ cm}^{-1}$ .

#### IV. FLUORESCENCE OF THE $C_{4v}$ CENTER

By exciting oxygen-free  $\text{CaF}_2:\text{Ce}^{3+}$  crystals at liquid-helium temperature with radiation in the B absorption band, fairly strong fluorescence has been produced in the wavelength region between 3130 and 3540  $\text{\AA}$ . Using the experimental setup described in Sec. II, attempts were made to find emission from each of the  $5d$  levels of the  $C_{4v}$  center. Sufficiently strong emission was obtained, however, only from the lowest  $5d$  level, the zero-phonon line of the B band, at  $31923 \text{ cm}^{-1}$ . The strongest emission occurred when the exciting light had a wavelength of about 3090  $\text{\AA}$ . Figure 7 shows a microphotometer tracing of a photographic recording of the fluorescent emission, and Table II lists the positions of the more important peaks.

Because the spin-orbit splitting of the  $4f$  levels is expected to be considerably greater than the crystal-field splitting, the fluorescence is expected to fall into two wavelength regions corresponding to the  $^2F_{5/2}$  and  $^2F_{7/2}$  levels of the free  $\text{Ce}^{3+}$  ion. The energy-level diagram for the  $C_{4v}$  center appears in Fig. 8. Two wavelength regions compa-

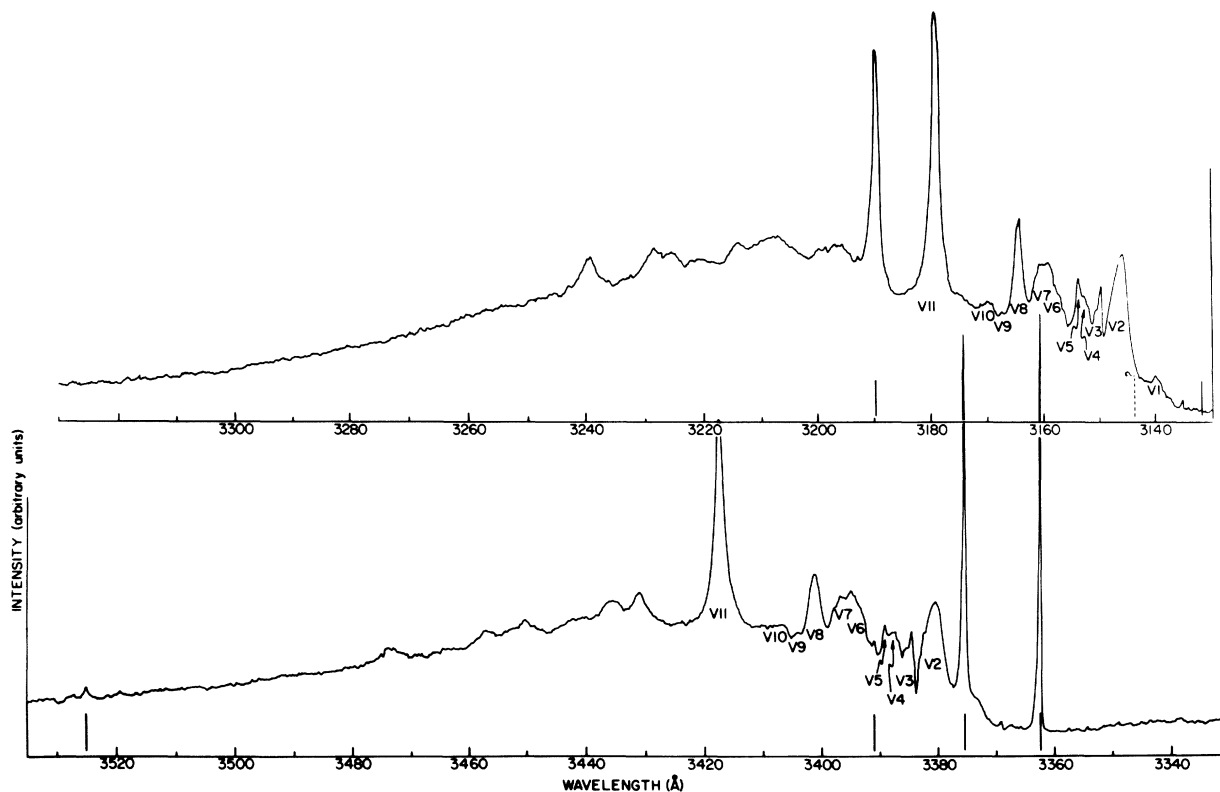


FIG. 7. Ultraviolet fluorescence at 2.2 K of No. 677  $\text{CaF}_2:\text{Ce}^{3+}$  (0.003 mole%) between 3130 and 3530 Å. Microdensitometer tracing of a photographic plate. The positions of the six zero-phonon lines observed are marked with solid vertical lines, and the estimated position of the one unobserved zero-phonon line is marked with a dashed vertical line. Components of the vibrational sidebands of the highest-energy lines in the  ${}^2F_{5/2}$  and  ${}^2F_{7/2}$  regions are labeled to agree with the corresponding lines in absorption shown in Fig. 6.

rable to those predicted are evident in the observed fluorescence (Fig. 7), where the  ${}^2F_{5/2}$  region is mainly between 3130 and 3250 Å, and the  ${}^2F_{7/2}$  region is mainly between 3360 and 3525 Å. Separation of the two regions is comparable to the free-ion value<sup>9</sup> of  $2253\text{ cm}^{-1}$ . Several of the fluorescence lines reported here have been observed before,<sup>3</sup> but there has previously been no attempt to discriminate carefully between purely electronic bands and vibrational sidebands, nor to establish the  $4f$  energy-level diagram.

The more apparent features of the spectrum in Fig. 7 are as follows: In the  ${}^2F_{5/2}$  region, there is a strong, structured vibrational sideband following the resonance line. The resonance line itself, however, is reabsorbed and consequently fails to appear, since the emitted light passed through the crystal on its way to the spectrograph. In addition, in the  ${}^2F_{5/2}$  region, a strong, fairly sharp line appears at 3189.5 Å. In the  ${}^2F_{7/2}$  region, besides the vibrational structures, the most prominent features are two strong, fairly sharp lines at 3362.5 and 3375.6 Å. Other zero-phonon

lines may be found by searching among the component peaks of the vibrational sidebands, and these are described below.

It is striking that the vibrational sidebands of the sharp (zero-phonon) lines in emission at 3189.5, 3362.5, and 3375.6 Å, as well as the reabsorbed resonance line at 3131.7 Å are identical to each other in spacing and (for the most part) in relative strengths of the several components, and agree equally well with the vibrational sideband of the absorption line at 3131.7 Å. The correspondence is emphasized in Figs. 6 and 7 by the labeling of the more prominent components (not a vibrational series) of the vibrational sidebands of the absorption line at 3131.7 Å and the emission lines at 3131.7 and 3362.5 Å. This constancy of the vibrational sidebands is very useful, in that weak lines due to purely electronic transitions can be picked out of what would otherwise be a confusing array of peaks.

By this procedure, and by comparing the emission of crystals of differing cerium concentration, the  $4f$  energy levels are determined as shown in Fig. 8. Some observed emission lines, in particu-

TABLE II. Prominent fluorescence peaks of  $\text{CaF}_2:\text{Ce}^{3+}$  (0.003 mole%) at liquid-helium temperature. Separations of zero-phonon lines from resonance line (at  $\sigma_g$ ) and of vibrational bands from their origin lines (at  $\sigma_0$ ).

Zero-phonon lines from $C_{4v}$ center (Fig. 8)	$\lambda$ (Å)	$\sigma$ ( $\text{cm}^{-1}$ )	$\sigma - \sigma_g$ ( $\text{cm}^{-1}$ )	$\sigma - \sigma_0$ ( $\text{cm}^{-1}$ )
${}^2F_{5/2}$				
$GE_{3/2}$ (assumed:	3131.7	31923)	0	0
	3146.0	31777		146
	3150.7	31730		190
	3151.0			
	3152.1			
	3153.6	31700		223
	3159.6	31640		283
	3164.7	31589		334
3179.3	31444		479	
$E_{5/2}E_{3/2}$	3189.5	31344	579	
${}^2F_{7/2}$				
$E_{1/2}E_{1/2}$ (not from $C_{4v}$ center	3362.5	29731	2192	
	3370)			
$GE_{3/2}$	3375.6	29616	2307	
	3380.8	29570		161
	3384.5	29535		195
	3384.8			
	3386.0			
3387.9	29508		223	
$GE_{1/2}$	3390.85	29482.7	2440	
	3392.0	29460		271
	3400.9	29395		336
	3417.5	29253		478
	3430.4			
$E_{5/2}E_{3/2}$	3525	28361	3562	

lar the one at 3370 Å, are attributed to  $\text{Ce}^{3+}$  centers other than the  $C_{4v}$  center by comparing them with approximate crystal-field calculations of the  $4f$  levels in the  $C_{4v}$  center.

In order to verify the assignments of the lines to the  $4f$  crystal-field states, the corresponding transition probabilities were calculated.<sup>8</sup> Use of the first-order (cubic-field)  $4f$  wave functions led to the results shown under "first-cubic calc." in Table III. These values agree fairly well with the observed line strengths except that the two lines of greatest wavelength are observed to be considerably weaker than those predicted. This discrepancy was removed by making a rather complete crystal-field analysis of the  $4f$  levels of the  $C_{4v}$  center.

In this analysis, the  $4f$  wave functions were obtained for the crystal-field states in a field of  $O_h$  symmetry. These appear, along with the energies in terms of  $B_0^4$  and  $B_0^6$ , in Table IV. The matrix of the  $C_{4v}$  crystal-field operator between these wave functions was then solved for the parameters  $B_0^4$ ,

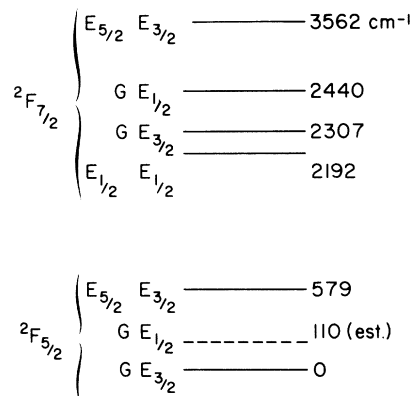


FIG. 8.  $4f$  crystal-field levels of the  $C_{4v}$  center of  $\text{CaF}_2:\text{Ce}^{3+}$ , obtained from the fluorescence of Fig. 7.

$B_0^4$ ,  $B_4^4$ ,  $B_0^6$ , and  $B_4^6$ , using the measured energy levels as known quantities. Since one of these levels (the second lowest) has not been observed, additional information in the form of measured  $g$  values<sup>19</sup> was employed. The resulting parameters and wave functions, characterizing the  $C_{4v}$  center, appear in Table V, along with orbital reduction factors  $k_x$  and  $k_z$ . These quantities are analogous to the single orbital reduction factor  $k$  introduced by Bleany,<sup>20</sup> and reflect the fact that there is a large axial perturbation of the outermost electron orbitals in the  $C_{4v}$  center. Another result of the analysis is the prediction that the second-lowest  $4f$  level,  ${}^2F_{5/2}GE_{1/2}$ , should lie at 110  $\text{cm}^{-1}$ .

From the wave functions of Table IV new transition probabilities were calculated. These appear under "exact calc." in Table III. The two lines of greatest wavelength are now predicted to be very weak, in good agreement with observation. The agreement of the predicted relative strengths of the other  ${}^2F_{7/2}$  lines,  $E_{1/2}E_{1/2}$  and  $GE_{3/2}$ , is also improved. It is interesting in the wave functions in Table V that the tetragonal perturbation mixes cubic-field states  $|{}^2F_{7/2}G \pm \frac{1}{2}\rangle$  and  $|{}^2F_{7/2}E_{1/2} \pm \frac{1}{2}\rangle$

TABLE III. Calculated relative line strengths of fluorescence from the  $5dGE_{3/2}$  level of the  $C_{4v}$  center.

Transition to	First-order calc. (wave functions for $O_h$ crystal field)	Exact calc. (wave functions for observed $C_{4v}$ crystal field)
${}^2F_{5/2}$ $GE_{3/2}$	1.00	1.00
	0.04	0.05
	0.27	0.27
${}^2F_{7/2}$ $E_{1/2}E_{1/2}$	0.64	1.04
	0.40	0.37
	0.32	0.02
	0.13	0.04

TABLE IV. Energies and wave functions of the  $j = \frac{5}{2}$  and  $j = \frac{7}{2}$  states of a  $4f$  electron in a crystal field of  $O_h$  symmetry.

State	Energy	Wave function
$j = \frac{7}{2} E_{5/2} \pm \frac{3}{2}$	$- \frac{18}{77} B_0^4 + \frac{20}{143} B_0^6$	$\frac{1}{2} \sqrt{3}   \frac{7}{2} \mp \frac{5}{2} \rangle - \frac{1}{2}   \frac{7}{2} \pm \frac{3}{2} \rangle$
$G \pm \frac{1}{2}$	$\left. \begin{array}{l} \frac{2}{77} B_0^4 - \frac{80}{429} B_0^6 \\ \frac{2}{11} B_0^4 + \frac{100}{429} B_0^6 \end{array} \right\}$	$\frac{1}{2} (\frac{7}{3})^{1/2}   \frac{7}{2} \pm \frac{7}{2} \rangle - \frac{1}{2} (\frac{5}{3})^{1/2}   \frac{7}{2} \mp \frac{1}{2} \rangle$
$G \pm \frac{3}{2}$		$\frac{1}{2}   \frac{7}{2} \mp \frac{5}{2} \rangle + \frac{1}{2} \sqrt{3}   \frac{7}{2} \pm \frac{3}{2} \rangle$
$E_{1/2} \pm \frac{1}{2}$	$\frac{2}{11} B_0^4 + \frac{100}{429} B_0^6$	$\frac{1}{2} (\frac{5}{3})^{1/2}   \frac{7}{2} \pm \frac{7}{2} \rangle + \frac{1}{2} (\frac{7}{3})^{1/2}   \frac{7}{2} \mp \frac{1}{2} \rangle$
$j = \frac{5}{2} E_{5/2} \pm \frac{3}{2}$	$- \frac{4}{21} B_0^4$	$\mp (\frac{1}{6})^{1/2}   \frac{5}{2} \mp \frac{5}{2} \rangle \pm (\frac{5}{6})^{1/2}   \frac{5}{2} \pm \frac{3}{2} \rangle$
$G \pm \frac{1}{2}$	$\left. \begin{array}{l} \frac{2}{21} B_0^4 \end{array} \right\}$	$  \frac{5}{2} \pm \frac{1}{2} \rangle$
$G \pm \frac{3}{2}$		$\pm (\frac{5}{6})^{1/2}   \frac{5}{2} \mp \frac{5}{2} \rangle \pm (\frac{1}{6})^{1/2}   \frac{5}{2} \pm \frac{3}{2} \rangle$

quite strongly, while it mixes  $| {}^2F_{7/2} E_{5/2} \pm \frac{3}{2} \rangle$  and  $| {}^2F_{7/2} G \pm \frac{3}{2} \rangle$  to only a very slight extent. The mixing of  $| {}^2F_{5/2} E_{5/2} \pm \frac{3}{2} \rangle$  and  $| {}^2F_{7/2} E_{5/2} \pm \frac{3}{2} \rangle$  is also fairly large.

#### V. ABSORPTION OF THE $C_{3v}$ CENTER

The differing symmetry of the  $Ce^{3+}$  center whose charge compensator is an interstitial  $F^-$  at  $(\frac{1}{2}a, \frac{1}{2}a, \frac{1}{2}a)$  makes the problems involved in the treatment of its crystal field quite different than those encountered in the above discussion of the  $C_{4v}$  center. Nevertheless, the two centers are so closely related, forming the first two of the series of  $Ce^{3+} : F_i^-$  centers in  $CaF_2$ , that it has been decided to include here what has been detected of the  $4f \rightarrow 5d$  transitions of the  $C_{3v}$  center. This consists of the observation, in the ultraviolet absorption of a few  $CaF_2 : Ce^{3+}$  crystals, of a very closely spaced pair of lines around  $3118.5 \text{ \AA}$  ( $32057 \text{ cm}^{-1}$ ), shown in Fig. 9. A few associated vibrational satellites,

as well as a hot band and the behavior of the pair of lines under uniaxial stress, have also been observed.

It is instructive to compare this  $C_{3v}$  center with the  $C_{3v}$  center arising from the presence of an  $O^{2-}$  ion substituting for one of the monovalent nearest neighbors of the  $Ce^{3+}$  ion, i. e., for a lattice fluoride ion at  $(\frac{1}{4}a, \frac{1}{4}a, \frac{1}{4}a)$ . See Fig. 10. This center produces<sup>3</sup> the closely spaced pair of zero-phonon lines in absorption at  $3383.5$  and  $3382.8 \text{ \AA}$  (separation  $6.1 \pm 0.5 \text{ cm}^{-1}$ ) along with a vibrational sideband with a moderate amount of structure, and occurs predominantly in  $CaF_2 : Ce^{3+}$  crystals grown in the presence of oxygen.

Crystal-field theory explains why the two lowest  $5d$  energy levels of both of these trigonal centers, corresponding to the  $e$  states of a  $d$  electron in a field of  $O_h$  (cubic) symmetry, are so closely spaced. On going to the double group  $O_h'$ , the doubly degenerate  $e$  states remain degenerate, becoming the fourfold degenerate  $eG$  states. On the other hand, reduction of symmetry in the single groups  $O_h \rightarrow C_{3v}$  gives  $e \rightarrow e$ , and thus also fails to remove the degeneracy of the  $e$  states. Only reduction of symmetry in the double groups produces a splitting, namely,  $eG \rightarrow eGE_{1/2} + eGE_{3/2}$ . This splitting is quite small, being a second-order effect depending upon the combined action of the spin-orbit coupling and of the lowering of site symmetry. Calculation of the splitting of the lowest  $4f$  levels,  ${}^2F_{5/2}G$  in the cubic crystal field, by a crystal field of  $C_{3v}$  symmetry, into  ${}^2F_{5/2}GE_{1/2} + {}^2F_{5/2}GE_{3/2}$  shows that this will also be fairly small. Even though the splitting is here a first-order effect, its value as a function of crystal-field parameters is the sum of two terms of comparable magnitude and opposite

TABLE V. Crystal-field parameters, orbital reduction factors, and wave functions of the  $4f$  levels of the  $C_{4v}$  center of  $CaF_2 : Ce^{3+}$ .

$B_0^2 = 339 \text{ cm}^{-1}$				
$B_0^4 = -2348 \text{ cm}^{-1}$			$k_x = 0.9840$	
$B_4^4 = -1734 \text{ cm}^{-1}$			$k_z = 0.9698$	
$B_0^6 = 990 \text{ cm}^{-1}$				
$B_4^6 = -1717 \text{ cm}^{-1}$				
$\left( \begin{array}{l}   \frac{7}{2} E_{5/2} E_{3/2} \pm \frac{3}{2} \rangle \\   \frac{7}{2} G E_{3/2} \pm \frac{3}{2} \rangle \\   \frac{5}{2} E_{5/2} E_{3/2} \pm \frac{3}{2} \rangle \\   \frac{5}{2} G E_{3/2} \pm \frac{3}{2} \rangle \end{array} \right)$	$= \left( \begin{array}{cccc} -0.00566 & 0.29465 & 0.03418 & -0.95498 \\ -0.00597 & 0.04463 & -0.99874 & -0.02194 \\ 0.01043 & 0.95453 & 0.03609 & 0.29574 \\ 0.99991 & -0.00802 & -0.00615 & -0.00863 \end{array} \right)$	$\left( \begin{array}{l}   \frac{5}{2} G \pm \frac{3}{2} \rangle \\   \frac{5}{2} E_{5/2} \pm \frac{3}{2} \rangle \\   \frac{7}{2} G \pm \frac{3}{2} \rangle \\   \frac{7}{2} E_{5/2} \pm \frac{3}{2} \rangle \end{array} \right)$		
$\left( \begin{array}{l}   \frac{7}{2} G E_{1/2} \pm \frac{1}{2} \rangle \\   \frac{7}{2} E_{1/2} E_{1/2} \pm \frac{1}{2} \rangle \\   \frac{5}{2} G E_{1/2} \pm \frac{1}{2} \rangle \end{array} \right)$	$= \left( \begin{array}{ccc} -0.05006 & -0.73718 & 0.67384 \\ -0.02627 & 0.67542 & 0.73696 \\ 0.99840 & -0.01919 & 0.05317 \end{array} \right)$	$\left( \begin{array}{l}   \frac{5}{2} G \pm \frac{1}{2} \rangle \\   \frac{7}{2} E_{1/2} \pm \frac{1}{2} \rangle \\   \frac{7}{2} G \pm \frac{1}{2} \rangle \end{array} \right)$		

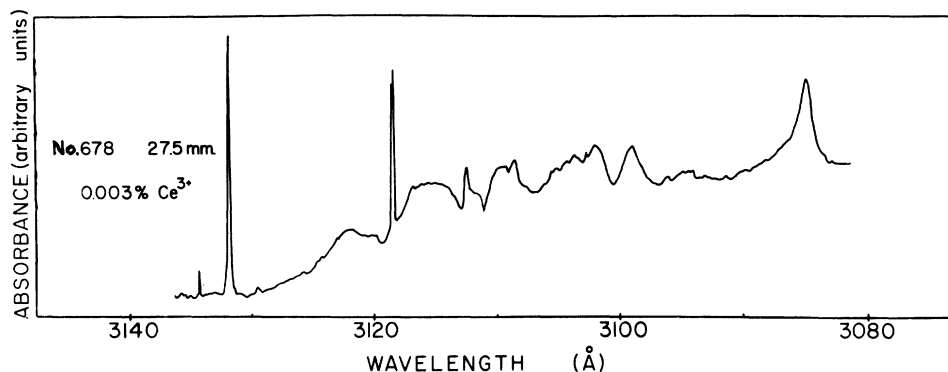


FIG. 9. Absorption spectrum as in Fig. 6, except that the  $C_{3v}(F_i^-)$  center was present in the crystal, producing the doublet observed at 3118.5 Å.

sign, so that the two states can lie close together and it will not be obvious which of them is to be lower.

Figure 11(a) shows the zero-phonon lines at 7.5 K of the lowest-energy  $4f \rightarrow 5d$  absorption of the  $C_{3v}(O_{\text{subs}}^{2-})$  center, as the  $C_{3v}$  oxide-compensated  $Ce^{3+}$  center will be called in what follows. As the temperature is gradually raised by the method described in Sec. II, hot bands of these lines begin to appear. They show up most clearly around 35.9 K, and are shown in Fig. 11(b) at that temperature. From the separation of the two pairs of lines, the second-lowest  $4f$  level is found to lie  $60.2 \pm 0.7 \text{ cm}^{-1}$  above the ground state.

The corresponding lowest-energy  $4f \rightarrow 5d$  absorption lines of the  $C_{3v}(F_i^-)$  center, as the  $C_{3v}$  interstitial-fluoride-compensated  $Ce^{3+}$  center will be called in what follows, are always observed superimposed on the absorption of the  $C_{4v}$  center, namely, on the second vibrational peak (V2) following the zero-phonon line at 3131.7 Å. Figure 12(a) shows this very closely spaced pair of lines at 3118.5 Å

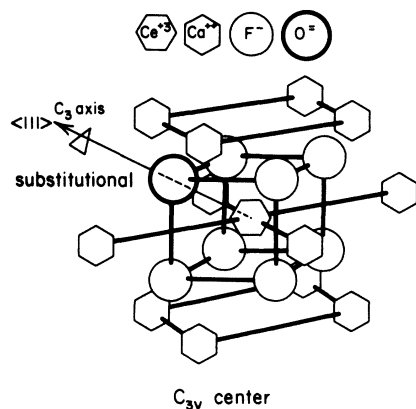


FIG. 10. The  $C_{3v}(O_{\text{subs}}^{2-})$  center of  $CaF_2:Ce^{3+}$ . Here an  $O^{2-}$  ion substitutes for one of the nearest-neighbor lattice  $F^-$  ions, and reduces the point symmetry of the  $Ce^{3+}$  ion to  $C_{3v}$ .

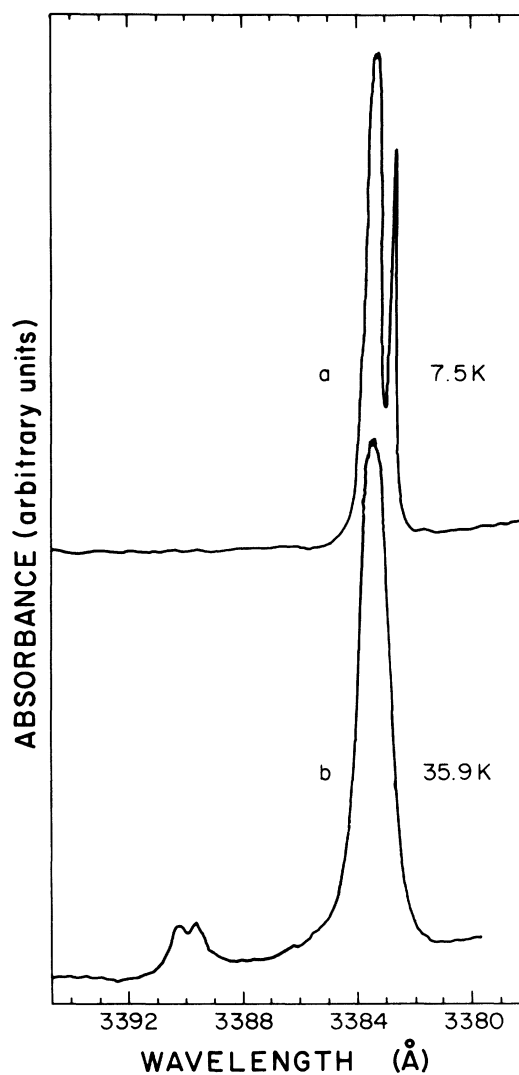


FIG. 11. Absorption spectra of No. 398  $CaF_2:Ce^{3+}$  (0.01 mole%), showing the effect of temperature on the closely spaced pair of lines attributed to the  $C_{3v}(O_{\text{subs}}^{2-})$  center. The hot bands are separated by  $60.2 \text{ cm}^{-1}$  from the low-temperature lines. Photoelectric tracings.

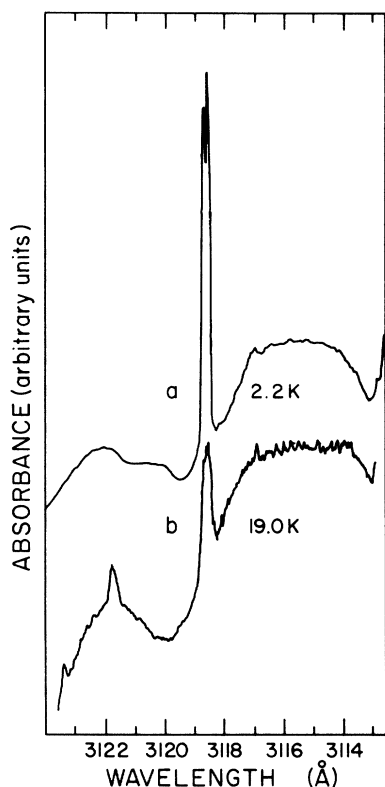


FIG. 12. Absorption spectra of (a) No. 678  $\text{CaF}_2:\text{Ce}^{3+}$  (0.003 mole%) and (b) No. 398  $\text{CaF}_2:\text{Ce}^{3+}$  (0.01 mole%), showing the effect of temperature on the very closely spaced pair of lines attributed to the  $C_{3v}(\text{F}_1^-)$  center. The hot band is separated by  $33.1 \text{ cm}^{-1}$  from the low-temperature lines; at the higher temperature neither pair is resolved. Photoelectric tracings.

at a temperature of 2.2 K, whose separation is about  $0.14 \text{ \AA}$  ( $1.4 \text{ cm}^{-1}$ ) and whose combined full width at half-maximum is about  $0.19 \text{ \AA}$  ( $2.0 \text{ cm}^{-1}$ ). A hot band starts to appear when the temperature exceeds about 10 K, and at 19.0 K its appearance is as shown in Fig. 12(b). The hot band lies directly on top of band VI, and of course cannot be resolved into its two components. From its separation from the low-temperature lines, the second-lowest  $4f$  level is found to lie about  $33.1 \text{ cm}^{-1}$  above the ground state.

Figure 13 shows the four experimentally determined energy levels of both of the  $C_{3v}$  centers. Kaplyanskii and Medvedev's analysis<sup>12</sup> of the electric field splittings of the lines around  $3383 \text{ \AA}$  arising from the  $C_{3v}(\text{O}_{\text{subs}}^{2-})$  center led them to assign the levels in the manner shown to the irreducible representations of the  $C_{3v}$  group. McLaughlan and Forrester confirmed by EPR<sup>21</sup> that the ground state here belonged to  $E_{1/2}$ , and interpreted the EPR data of Weber and Bierig<sup>22</sup> to assign the ground

state of the  $C_{3v}(\text{F}_1^-)$  center to  $E_{3/2}$ , as shown in Fig. 13. Combining the resulting reversal in the order of the two lowest  $4f$  states with the observed reversal in intensity of the absorption lines in Figs. 11(a) and 12(a), the order of the  $5d$  states is deduced to be the same in the two  $C_{3v}$  centers, and they are labeled accordingly in Fig. 13.

In order to verify that the lines at  $3118.5 \text{ \AA}$  could arise from a  $\text{Ce}^{3+}$  center of trigonal symmetry, their behavior under the action of uniaxial stress was examined. Since strain in any direction other than one of the three  $\langle 001 \rangle$  directions will produce pseudosplitting in a trigonal center, it was decided to apply stress in this direction to simplify the observations. Figure 14 shows microdensitometer tracings of photographic records of the spectra in the region of interest. The sample, held below 2.2 K, was subjected to progressively greater stresses up to 2379 atm, acting along one of the  $\langle 001 \rangle$  directions, using the procedure described in Sec. II.

The separation of the two lines at zero stress is seen to increase as stress is applied, while no definite splitting can be detected. The right-hand line of the pair in question shifts to the left only by an extremely small amount, too small to be seen in Fig. 14 or to be measured accurately, while remaining quite sharp. The left-hand line

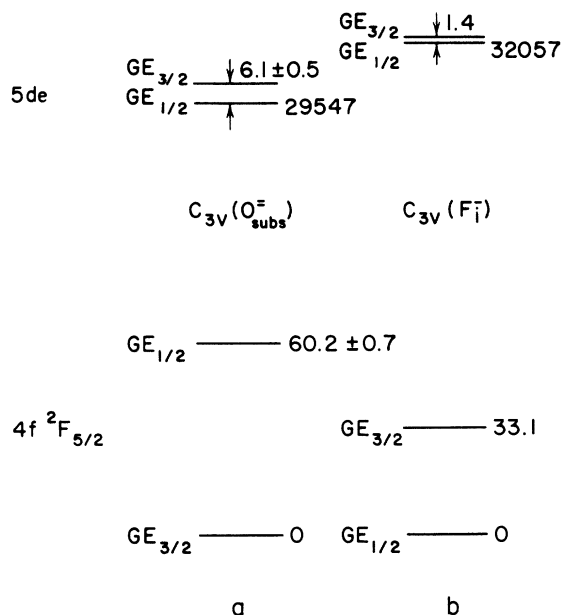


FIG. 13. Energy levels of the two lowest  $4f$  states ( ${}^2F_{5/2}GE_{3/2}$  and  ${}^2F_{5/2}GE_{1/2}$ ) and the two lowest  $5d$  states ( $eGE_{3/2}$  and  $eGE_{1/2}$ ) of the two trigonal centers of  $\text{CaF}_2:\text{Ce}^{3+}$ . Wave numbers are given in  $\text{cm}^{-1}$ . (a) The  $C_{3v}$  center with a substitutional  $\text{O}^{2-}$  charge compensator at  $(\frac{1}{2}a, \frac{1}{2}a, \frac{1}{2}a)$ . (b) The  $C_{3v}$  center with an interstitial  $\text{F}^-$  charge compensator at  $(\frac{1}{2}a, \frac{1}{2}a, \frac{1}{2}a)$ .

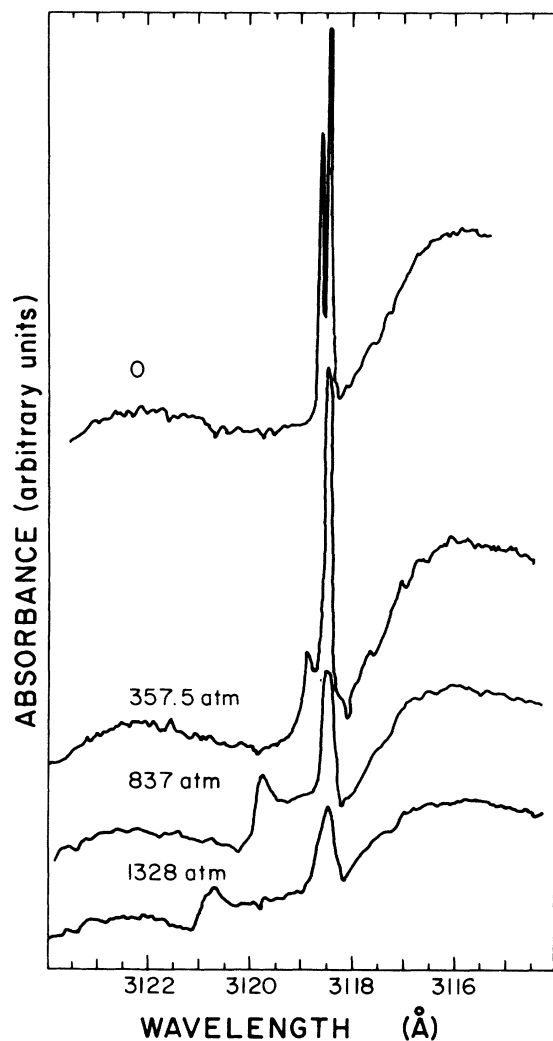


FIG. 14. Effect of uniaxial strain along a  $\langle 001 \rangle$  direction on the sharp lines near  $3118.5 \text{ \AA}$ . Separation of the two lines increases with strain, but neither line unambiguously shows any further splitting. The broadbands around  $3122$  and  $3116 \text{ \AA}$  are vibrational satellites of the sharp line at  $3131.7 \text{ \AA}$ . Microdensitometer tracings of photographic records of the absorption spectrum of No. 677  $\text{CaF}_2 : \text{Ce}^{3+}$  (0.003 mole%) at  $2.2 \text{ K}$ .

shows a decided shift to the left, at a rate of about  $1.63 \times 10^{-3} \text{ \AA/atm}$ , before becoming too diffuse to be detected above a stress of about  $2000 \text{ atm}$ . The slight appearance of splitting at stresses above about  $1100 \text{ atm}$ , especially in the left-hand line, presumably results from experimental error, such as slight imperfections in the flatness or parallelness of the faces of the crystal, or rotation about a horizontal axis of the steel anvils pressing on the crystal. Broadening of the  $C_{4v}$  line at  $3131.7 \text{ \AA}$  shows that such processes can be quite strong here. This line should show a pseudosplitting

under uniaxial stress along a  $\langle 001 \rangle$  direction into two components, with the component to the left about one-half as strong as its partner. The fact that this splitting is not as distinct as Kaplyanskii and Medvedev observed<sup>14</sup> indicates that some experimental error is probably acting here.

Although it would be preferable to examine the action on the lines at  $3118.5 \text{ \AA}$  of uniaxial stress in other directions, the observations described are probably consistent with their assignment to a center of trigonal symmetry. This observation, along with the intensity of the lines, their position, and their very small separation, supports the belief that they originate in the  $C_{3v}$  center illustrated in Fig. 3.

## VI. SUMMARY AND CONCLUSIONS

The general problem under study is how the  $\text{CaF}_2$  crystal interacts with the  $\text{Ce}^{3+}$  impurity ions introduced into it. That is, one uses the  $\text{CaF}_2$  as the source of a crystal field perturbing the electronic states of the  $\text{Ce}^{3+}$  ion, and from these perturbations one gains insight into the nature of the interaction. Much of the required investigation concerns the assignment of particular spectral lines to particular cerium centers. The present paper deals with the centers where the host lattice is strongly affected not only by the  $\text{Ce}^{3+}$  impurity ion, but also by a nearby interstitial  $\text{F}^-$  ion lying in the direction of either one of the  $C_4$  or one of the  $C_3$  axes of the host crystal, and with  $\text{Ce}^{3+}-\text{F}_i^-$  separation of approximately  $\frac{1}{2}a$  or  $\frac{1}{2}\sqrt{3}a$ , respectively. A future paper will describe the spectra of other centers, including the cubic  $\text{Ce}^{3+}$  center in  $\text{CaF}_2$ , where only the almost undisturbed  $\text{CaF}_2$  lattice ions are responsible for the crystal field, which is, as a result, at its simplest and most symmetric. Comparison of this crystal field with those of centers with lower symmetry elucidates the action of the charge compensators involved.

Here we have examined first the absorption bands of the  $\text{Ce}^{3+} : \text{F}_i^-$  center of  $C_{4v}$  symmetry in order to correlate them with its  $5d$  energy levels. The splitting, by the cubic part of the  $C_{4v}$  crystal field, of the  $5d$  states into  $e$  and  $t_2$  states is seen to amount to about  $17000 \text{ cm}^{-1}$ . Further splitting of the  $t_2$  states by the low-symmetry part of the  $C_{4v}$  crystal field gives rise to the E, F, and G bands. Even though only one of the expected two  $e$  levels can be identified, it is possible to compute the results given in Table I, namely, a partial set of crystal-field parameters of the  $C_{4v}$  field, along with a spin-orbit parameter different from its free-ion value.

The calculated value of  $B_0^4 = -36600 \text{ cm}^{-1}$  ( $\equiv -21Dq$ ) compares quite favorably with Loh's value<sup>23</sup> for  $\text{CaF}_2 : \text{Eu}^{2+}$  of  $B_0^4 = -35700 \text{ cm}^{-1}$ . The  $\text{Eu}^{2+}$  ions in that system probably occupied sites of

cubic symmetry. Agreement is also good with the value found<sup>24</sup> for  $\text{CaF}_2 : \text{Ce}^{3+}$  of  $B_0^4$  between  $-16\,800$  and  $42\,000\text{ cm}^{-1}$ , but not with Loh's result<sup>7</sup> of  $B_0^4 = -25\,200\text{ cm}^{-1}$  for the system under consideration here, the  $C_{4v}$  center of  $\text{CaF}_2 : \text{Ce}^{3+}$ .

Also reported here is a complete emission spectrum at liquid-helium temperature and at high resolution from a crystal of low cerium concentration, and accordingly arising predominantly from the  $C_{4v}$  center. Lines attributable to purely electronic  $5d \rightarrow 4f$  transitions of this center have been picked out of the considerable amount of fine structure thus obtained, so that energy levels have been assigned to six of the seven  $4f$  states.

Using these energies, along with some EPR data, it has been possible to solve completely the crystal-field problem for the  $4f$  levels of the  $C_{4v}$  center. One thus obtains the crystal-field parameters, orbital-reduction factors, and wave functions of Table V. A check on the reliability of these quantities, and on the assignments of the energy levels to specific crystal-field states, is provided by comparing calculated transition probabilities with the observed line strengths. This comparison is illustrated in Table III, where it can be seen that the transition probabilities calculated from the "exact" wave functions represent at least a great improvement over those calculated from the first-order wave functions in Table IV.

In particular, the complete calculation substantially increases the predicted strength of the transition to the  ${}^2F_{7/2}E_{1/2}E_{1/2}$  level—by about 60%—while those to the  ${}^2F_{7/2}GE_{1/2}$  and  ${}^2F_{7/2}E_{5/2}E_{1/2}$  levels are substantially reduced—by about 90 and 70%, respectively. The predicted transition probability of the transition to the  ${}^2F_{5/2}GE_{1/2}$  level, representing the line which has not been observed, remains just about as small. The agreement is good enough on the whole to lend considerable support

to the assignments of the lines in Fig. 8, and thereby to the proposed solution of the crystal-field problem.

Finally, arguments have been given for the assignment of the pair of lines at  $3118.5\text{ \AA}$  to the lowest-energy  $4f \rightarrow 5d$  transitions of the  $C_{3v}(F_i^-)$  center of  $\text{CaF}_2 : \text{Ce}^{3+}$  as shown in Fig. 3. This assignment is supported by the observed behavior of the lines under a uniaxial stress along a  $\langle 001 \rangle$  direction, but even more strongly by the comparison of these lines and their hot bands with the corresponding absorption of the  $C_{3v}(O_{\text{subs}}^{2-})$  center of  $\text{CaF}_2 : \text{Ce}^{3+}$ .

Absorption spectra will be described in later papers of this series of  $\text{Ce}^{3+}$  impurity centers in  $\text{CaF}_2$  other than the  $C_{4v}$  and  $C_{3v}$  centers with interstitial- $F^-$  ion charge compensation. Although no attempt has been made yet to observe fluorescence from these other centers, it would be very informative and not particularly difficult to do so. Transitions in these other centers are presumably responsible for the sharp lines reported here in fluorescence at  $3314.3$ ,  $3316.0$ ,  $3370$ , and  $3509.0\text{ \AA}$ , noticeable for the most part in crystals of higher cerium concentration. Comparison of the fluorescence from a series of crystals of increasing cerium concentration would be especially valuable.

#### ACKNOWLEDGMENTS

The author is indebted to D. S. McClure, under whose guidance this work was undertaken, for his constant interest and much helpful advice throughout its course. Thanks are due to H. Temple of the David Sarnoff Laboratories of RCA for growing the crystals used in this study, and to the Chemistry Department of Princeton University, whose facilities the author used as a visiting student.

\*Presented as a thesis to the Department of Physics, The University of Chicago, in partial fulfillment of the requirements for the Ph.D. degree. Research supported by the Office of Naval Research and the National Science Foundation.

<sup>†</sup>Present address: Institute for Medical Research, Camden, N. J. 08103.

<sup>1</sup>Gerhard H. Dicke, in *International Conference on Paramagnetic Resonance*, edited by W. Low (Academic, New York, 1963), p. 237.

<sup>2</sup>D. N. Batchelder and R. O. Simmons, *J. Chem. Phys.* **41**, 2324 (1964).

<sup>3</sup>A. A. Kaplyanskiĭ, V. N. Medvedev, and P. P. Feofilov, *Opt. Spektrosk.* **14**, 664 (1963) [*Opt. Spectrosc.* **14**, 351 (1963)]; P. P. Feofilov, *Opt. Spektrosk.* **6**, 234 (1959) [*Opt. Spectrosc.* **6**, 150 (1959)].

<sup>4</sup>J. M. Baker, E. R. Davies, and J. P. Hurrell, *Proc. R. Soc. A* **308**, 403 (1968). These authors demonstrated that the  $\text{Ce}^{3+}$  ion in the  $C_{4v}$  center of  $\text{CaF}_2 : \text{Ce}^{3+}$  shifts toward the interstitial  $F^-$  charge compensator ( $F_i^-$ ) by about  $0.025a$ , while each of the eight nearest-neighbor lattice  $F^-$  ions surrounding the  $F_i^-$  ion

shift toward it by about 10% of the  $F^- - F_i^-$  separation.

<sup>5</sup>Richard S. Meltzer, Ph.D. thesis (University of Chicago, 1968) (unpublished).

<sup>6</sup>The closely analogous absorption spectrum of the  $\text{Ce}^{3+}$  ion at a site of tetragonal symmetry in crystals of hydrogenated  $\text{CaF}_2 : \text{Ce}^{3+}$ , where the charge compensator is an interstitial  $H^-$  or  $D^-$  ion, was reported by I. T. Jacobs, G. D. Jones, K. Ždánký, and R. A. Satten [*Phys. Rev. B* **3**, 2888 (1971)]. They expected the absorption to the second-lowest  $5d$  level, the upper component of the  $e$  level, to appear in the  $3000\text{-\AA}$  region, that is, roughly  $3900\text{ cm}^{-1}$  above the lowest  $5d$  level. As in the present paper, attempts to locate this absorption were unsuccessful, and this fact was attributed to its low transition probability or to its being a broad line.

<sup>7</sup>Eugene Loh, *Phys. Rev.* **154**, 270 (1967).

<sup>8</sup>W. J. Manthey, Ph.D. thesis (University of Chicago, 1972) (unpublished).

<sup>9</sup>R. J. Lang, *Can. J. Res. A* **13**, 1 (1935); *Can. J. Res. A* **14**, 127 (1936).

<sup>10</sup>Frank Herman and Sherwood Skillman, *Atomic Structure*

- Calculations* (Prentice-Hall, Englewood Cliffs, N.J., 1963).
- <sup>11</sup>J. Wagner and S. Mascarenhas, *Phys. Rev. B* **6**, 4867 (1972).
- <sup>12</sup>A. A. Kaplyanskii and V. N. Medvedev, *Opt. Spektrosk.* **23**, 743 (1967) [*Opt. Spectrosc.* **23**, 404 (1967)].
- <sup>13</sup>A. A. Kaplyanskii and V. N. Medvedev, *Opt. Spektrosk.* **18**, 803 (1965) [*Opt. Spectrosc.* **18**, 451 (1965)].
- <sup>14</sup>M. H. Crozier, *Phys. Rev.* **137**, A1781 (1965).
- <sup>15</sup>J. M. Baker, E. R. Davies, and J. P. Hurrell, *Phys. Lett. A* **26**, 352 (1968); D. Kiro, W. Loh, and A. Kafri, *Phys. Rev. Lett.* **22**, 893 (1969).
- <sup>16</sup>J. M. Baker, W. Hayes, and D. A. Jones, *Proc. Phys. Soc. Lond.* **73**, 942 (1959).
- <sup>17</sup>Richard H. Heist and Francis K. Fong, *Phys. Rev. B* **1**, 2970 (1970).
- <sup>18</sup>R. W. Bierig, M. J. Weber, and S. I. Warshaw, *Phys. Rev.* **134**, A1504 (1964).
- <sup>19</sup>S. D. McLaughlan, *Phys. Rev.* **160**, 287 (1967).
- <sup>20</sup>B. Bleany, *Proc. R. Soc. A* **277**, 289 (1964).
- <sup>21</sup>S. D. McLaughlan and P. A. Forrester, *Phys. Rev.* **151**, 311 (1966).
- <sup>22</sup>M. J. Weber and R. W. Bierig, *Phys. Rev.* **134**, A1492 (1964).
- <sup>23</sup>Eugene Loh, *Phys. Rev.* **184**, 348 (1969).
- <sup>24</sup>R. C. Alig, Z. J. Kiss, J. P. Brown, and D. S. McClure, *Phys. Rev.* **186**, 276 (1969).